Electronic Supplementary Information

Hollow TiN nanotrees derived from a surface-induced Kirkendall effect and the application in high-power supercapacitors

Wei Wen,[*ac] Jincheng Yao,[a] Hua Tan[c] and Jin-Ming Wu[*b]

[a]College of Mechanical and Electrical Engineering, Hainan University, Haikou 570228, P. R. China.

[b]State Key Laboratory of Silicon Materials and School of Materials Science and Engineering, Zhejiang University, Hangzhou 310027, P. R. China.

[c]School of Physical and Mathematical Sciences, Nanyang Technological University, Singapore 637371 , Singapore.
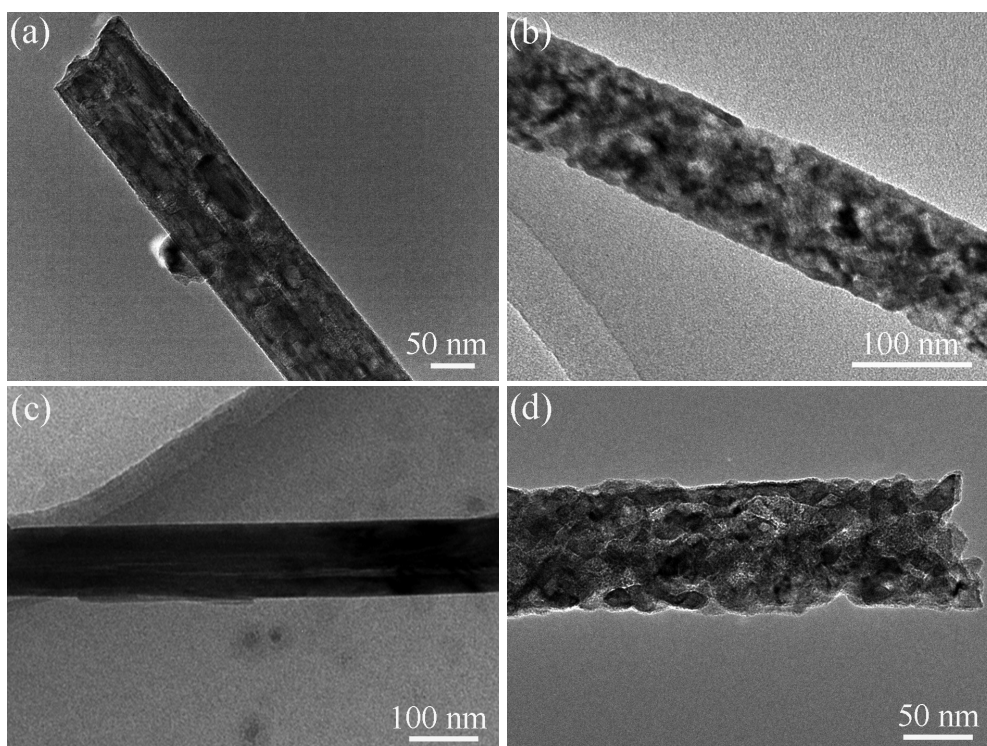
Fig. S1 (a,c) TEM images of TiO$_2$ and titanate nanowires;
and (b,d) the corresponding TiN nanowires after ammonia calcination.
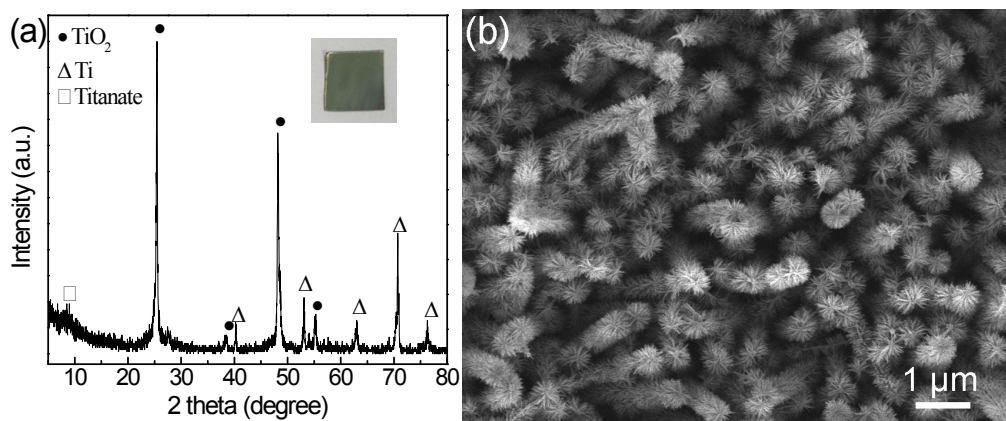
Fig. S2 Characterizations of TiO$_2$/titanate nanotrees.

(a) XRD pattern (inset: the corresponding photograph);

(b) FESEM image.

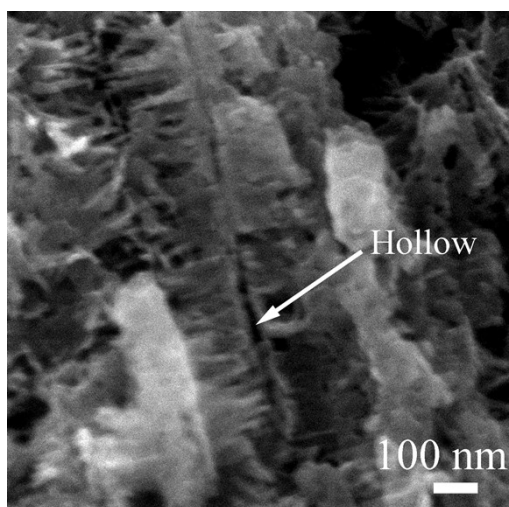The weak titanate peak in the XRD is due to their low crystallinity and small thickness.

Hollow

100 nm

Fig. S3 A cross-sectional FESEM image showing one hollow TiN nanotree.
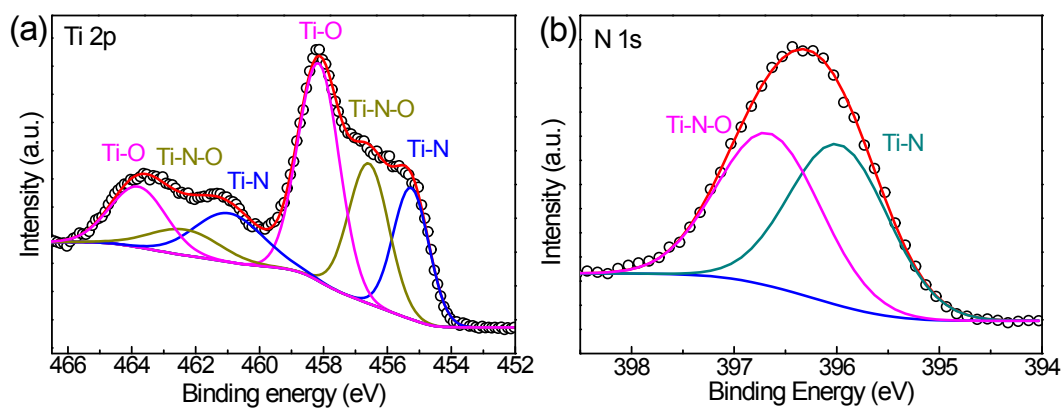
Fig. S4 XPS spectra of hollow TiN nanotrees.

(a) High-resolution Ti 2p spectrum;

(b) High-resolution N 1s spectrum.

The Ti-O and Ti-N-O peaks are due to unavoidable oxidation when exposed to air.
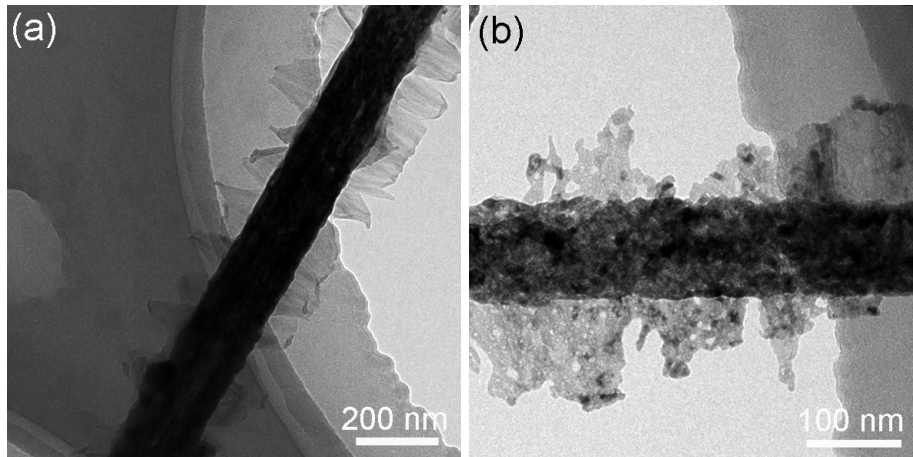
Fig. S5 Control sample of TiO$_2$/titanate nanotrees with less-dense branches.

(a) TEM image;

(b) the corresponding TiN nanotrees after nitridation.

Preparation processes of the control sample of TiO$_2$/titanate nanotrees with less-dense branches: the synthesis processes are similar to those in the Section 2.1 in the main text, except that 150 mL H$_2$O$_2$ aqueous solution (30%), instead of 50 mL, was used for preparing a relatively dilute deposition solution.
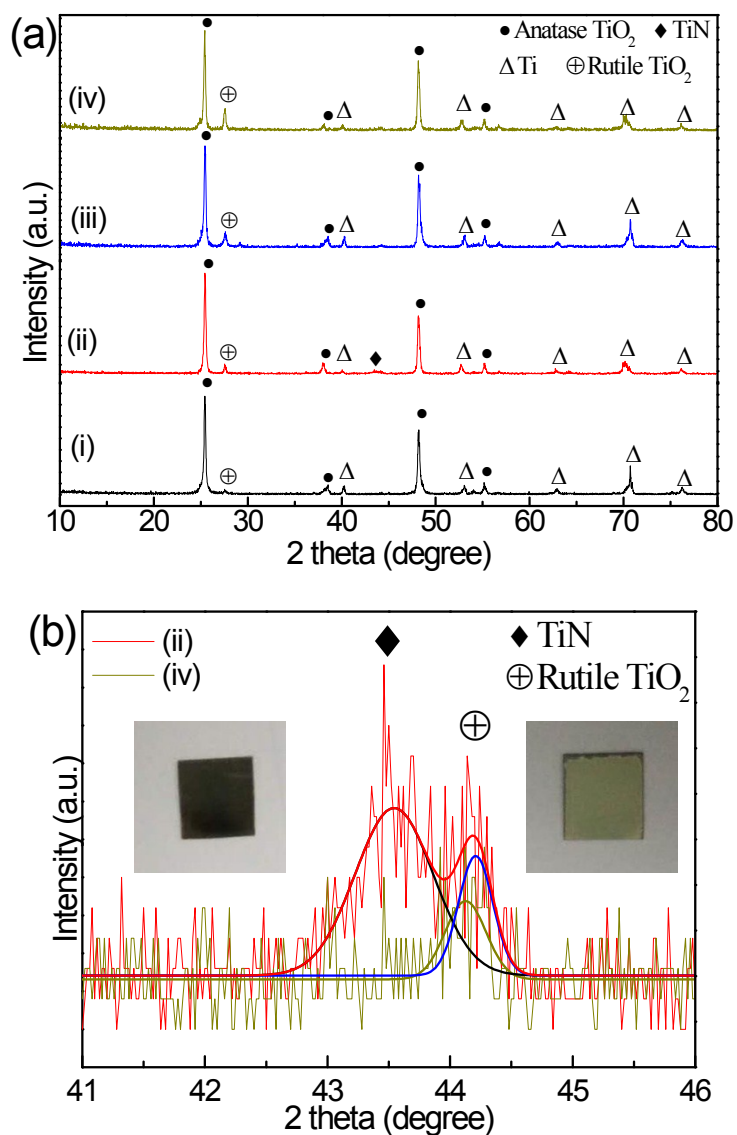
Fig. S6 Control experiments to verify the difference in reaction rates.

(a) XRD patterns of different samples. (i) Branched TiO_2 nanotrees (obtained by annealing TiO_2/titanate nanotrees at 400 °C in air), and (ii) after calcination in NH_3 at 800 °C for 10 min; (iii) TiO_2 nanowires, and (iv) after calcination in NH_3 at 800 °C for 10 min. Note that the complete conversion reaction takes 2 hr.

(b) Zoom-in view of the spectrum (ii) and (iv) and fitting results. The insets show the corresponding photographs (left for ii, right for iv).
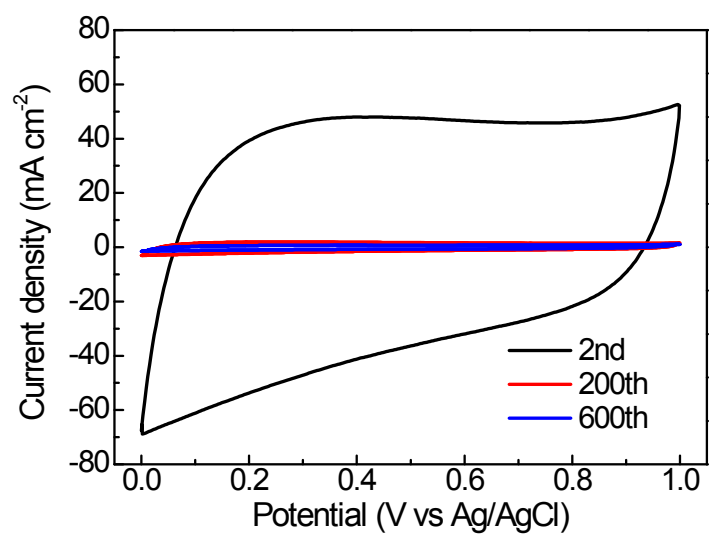
Fig. S7 CVs of the hollow TiN nanotrees in 0.5 M H_2SO_4 at different cycles at 500 mV s^{-1}.
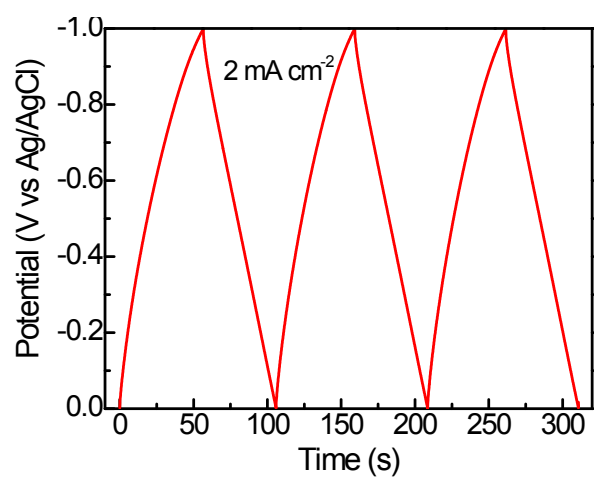
Fig. S8 Galvanostatic charge/discharge curve of hollow TiN nanotrees as a negative electrode at 2 mA cm^{-2} in a standard three-electrode system.
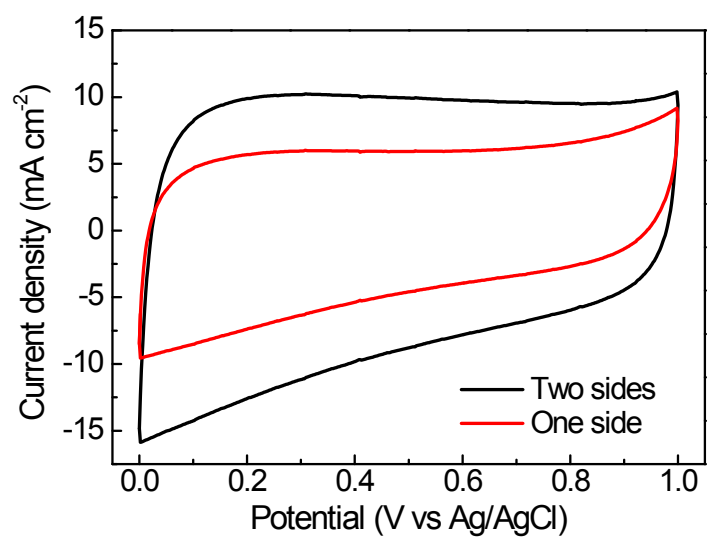
Fig. S9 CVs of the hollow TiN nanotrees with one side or two side films in 0.5 M H₂SO₄ at 100 mV s⁻¹.
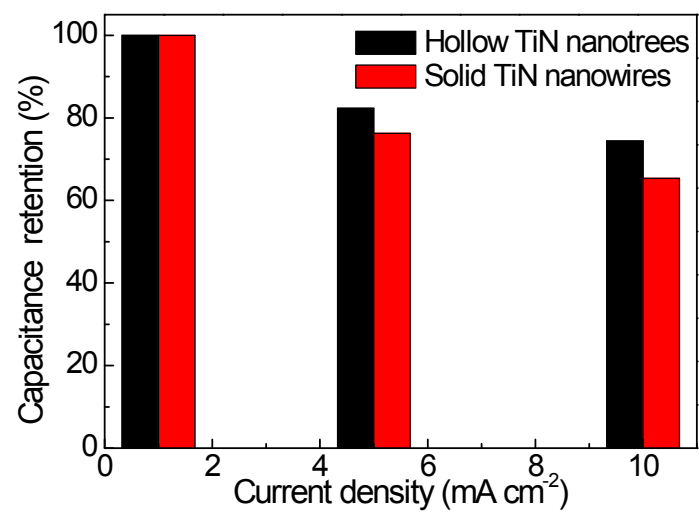
Fig. S10 Rate performance of hollow TiN nanotrees and TiN nanowires as positive electrode in a standard three-electrode system. Electrolyte: 1 M Li_2SO_4 aqueous solution.
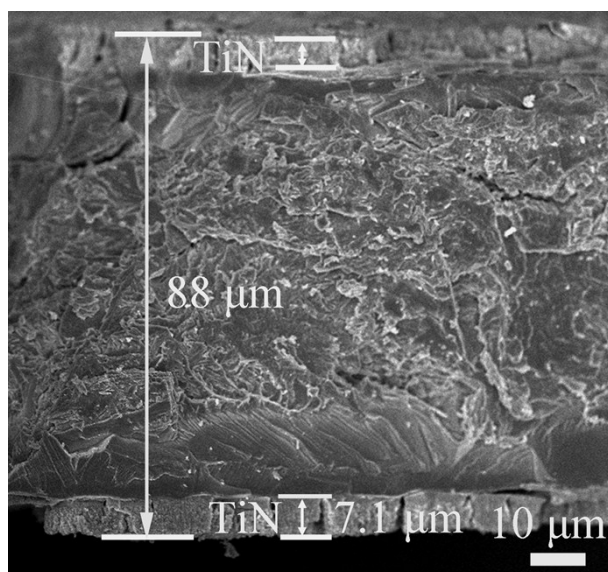
Fig. S11 Cross-section FESEM image showing the thickness of a whole electrode and the active material (TiN) layer.
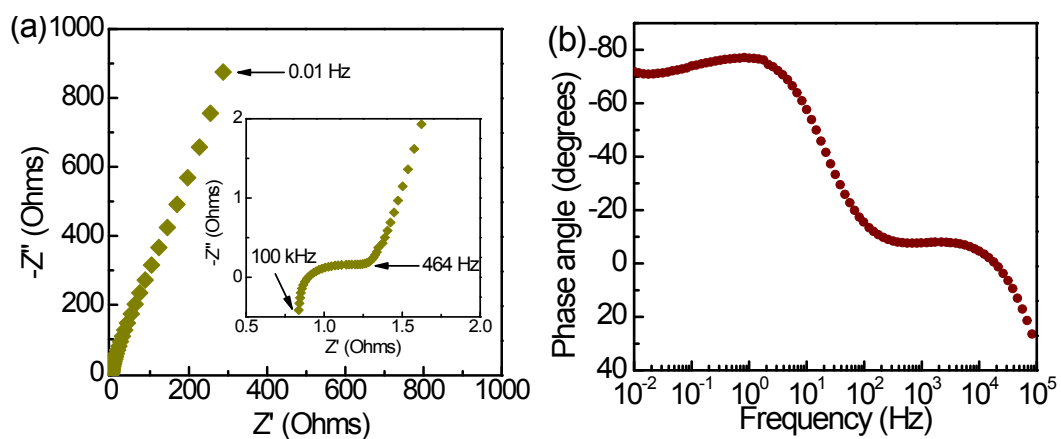
Fig. S12 (a) Nyquist plots of the symmetric supercapacitor device in discharge state (at the open circuit potential of about 0.35 V) over the frequency range from 100 kHz to 0.01 Hz. The inset shows the expanded view in the high frequency region.
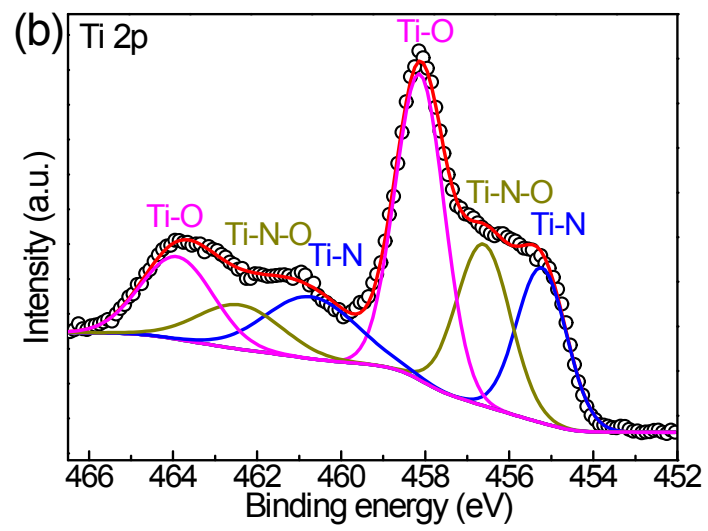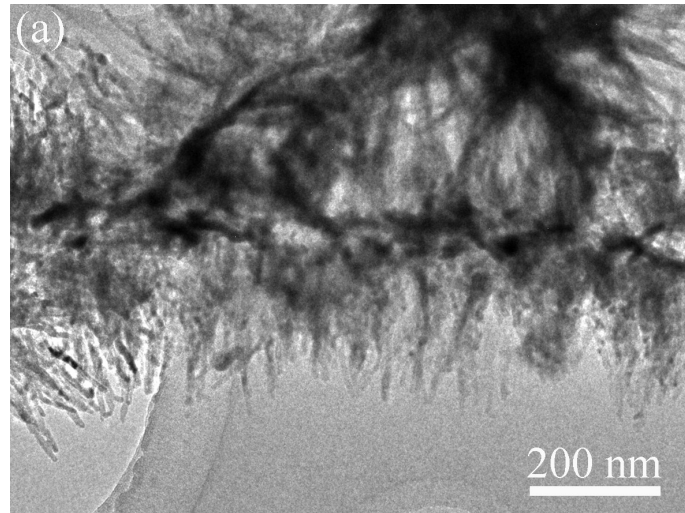(b) Impedance phase angle versus frequency. The -45° phase angle occurs at ~18.5 Hz.

Fig. S13 (a) TEM image;

(b) Ti 2p XPS spectrum of the electrode of the device after 350,000 cycles.